كلية الهندسة بشبرا
FACULTY OF ENGINEERING AT SHOUBRA
ERJ
PRINT ISSN 3009-6049
ONLINE ISSN 3009-6022

ENGINEERING RESEARCH JOURNAL (ERJ)
Volume (54),Issue (2)
April 2025, pp:27-37
https://erjsh.journals.ekb.eg

Behavior of Light Weight Reinforced Concrete Deep Beams with Polypropylene Fibers.

Ahmed Mohamed Abd-ELrahem [1,*],Ahmed Mahmoud [2],Mohammed Hisham [2],Tarek S. Mustafa [2]

[1] Department of Civil Engineering, Higher Institute of Engineering, 15th of May City, Cairo, Egypt.
[2] Department of Civil Engineering, Faculty of Engineering at Shoubra, Benha University, Cairo, Egypt.
**Corresponding author*

E-mail address: am01097978425@gmail.com, ahmed.ahmed@feng.bu.edu.eg, mohamed.abdelkreem@feng.bu.edu.eg, Tarek.mohamed@feng.bu.edu.eg

Abstract: The main objective of this research is to study the influence of polypropylene fibers on the behavior of lightweight concrete (LWC) deep beams with low and normal concrete grades. In addition, it is to investigate the main role of polypropylene fibers on the concrete material properties and the shear capacity of deep beams. Furthermore, it is to study the effect of some variable parameters on structural behavior to improve stiffness, ductility, crack width, and ultimate load capacity. The paper explores the impact of nine parameters on the behavior as: (1) volume of fiber (Vf = 0%, 0.1%, 0.05%, and 0.2%); (2) fiber aspect ratio (L_f/Φ_f = 26, 42 and 68); (3) longitudinal reinforcement ratio (μ/μ_{max} = 0.3,0.4 and 0.5). Finally, a comparison between experimental results and nonlinear finite element predictions using ANSYS V15 was performed. The testing results indicate that polypropylene fibers have been shown to significantly enhance the properties of lightweight concrete (LWC), with increases in compressive strength, tensile strength, and overall performance by 10.5%, 6.5%, and 10.75%, respectively. Additionally, both deformation resistance and workability of the concrete were notably improved. The comparison between experimental and numerical results demonstrated a strong correlation, with mean values for cracking load, ultimate load, and deflection at ultimate load closely aligning, achieving agreement rates of 95.98%, 100.72%, and 102.15%, respectively.

Keywords: Light-weight; RC deep Beams; Fibers; Nonlinear finite element; Simulation Modal .

1. Introduction

The mechanical properties of Polypropylene fiber-reinforced lightweight concrete are influenced by fiber dimensions and volume, concrete matrix properties, curing conditions, environmental factors, loading and mixing rates, and the specific type of lightweight concrete used. In general, the concrete mix was designed in accordance with the guidelines and specifications of both the applicable Egyptian Code (ECP) [1] and the American Concrete Institute (ACI) [2] standards guidelines. Although there are steel bars, concrete is very good in resisting compressive stress, but it is weak in tension stress and cracking resistance. Therefore, fiber is added to concrete to reduce the widening of the cracks and improve concrete's load-bearing capacity, and mechanical properties such as shear capacity, compressive strength, tensile strength, flexural strength, stiffness, and ductility [3, 4].

Polypropylene fibers, a new-generation chemical fiber, are produced on a large scale and rank fourth in production volume after polyesters, polyamides, and acrylics [5]. In 2012, Bagherzadeh [6] used different lengths of Polypropylene fibers (PPF) in lightweight concrete with a length [6mm and 12mm] proportions with 0.15% and 0.35% by cement weight. The results showed that the fibers with a length of 12mm give better results than fibers with a length of 6mm in compression and tensile strength. On the other hand, the samples (PPF) with longer lengths showed that better flexural strength was obtained compared to specimens with shorter fibers [6, 7]. Studies on the flexural behavior of fiber-reinforced concrete beams have shown that Polypropylene fibers enhance flexural performance. Specifically, the use of Polypropylene fibers and silica fumes in concrete resulted in an estimated 40% increase in flexural strength [8]. Fiber addition to concrete reduces strain and improves stress [9]. The polypropylene fibers improved the flexural strength of concrete and have good ductility, preventing cracks but had a slight effect on compression strength [10].

Extensive research exists on the mechanical properties of both high-strength and normal-strength reinforced concrete, with and without fibers, under various loading conditions. The addition of fibers to concrete decreases concrete bleeding and improves abrasion resistance, controls crack, increases tensile strength, and durability, and enhances the deformation properties [11-15]. The increased embedded depth of longer fibers likely explains this, as it increases the ultimate bond strength and resistance to fracture during pullout from the concrete matrix [16]. Compared to straight fibers, increasing the fiber content or aspect ratio significantly improves energy absorption capacity and ductility. Notably, deformed fibers with hooked ends provide greater toughness. Fibers with high aspect ratios are particularly effective in enhancing post-peak performance, attributed to their strong resistance to pullout from the matrix [17]. Reinforced foamed lightweight concrete beams and slabs have been investigated and compared with normal-weight concrete beams and slabs. The results of the study

made by Lee, Yee Ling et al., [4] showed that lightweight foamed concrete beams and slabs were weak in resisting shear and failed in flexure. It was reported that the failure in flexure shear occurred due to the absence of coarse aggregate in lightweight foamed mortar. The brittleness of lightweight concrete can be minimized by using steel reinforcement such as normal concrete. [18-23].

2. Experimental program

2.1 Description of tested beams

Eight lightweight deep beam specimens with a rectangular cross-section, 800 mm overall depth, 150 mm width, 2200 mm total length, and 2000 mm clear span made up the experimental program. The beam's total length was divided into five sections, with the end sections significantly reinforced to ensure against failure during testing, as indicated in Fig. 1. The middle section, measuring 400 mm, was the tested zone (pure flexure). The two shear spans measured 800 mm. As presented in Table 1, the eight tested deep beams were classified into four distinct groups: A, B, C, and D. Group A consists of two control deep beams: the second deep beam (B2) has polypropylene fiber, whereas the first deep beam (B1) is a control deep beam without it. Groups B, C, and D contain six deep beams with different volume contents, aspect ratios of polypropylene, and main steel reinforcement ratios, as shown in Table (1). Concrete mechanical properties are listed in Table 2, and reinforcement steel properties are detailed in Table 3 and Figure 2. All beams used 16 mm diameter steel bars in the tension zone and 10 mm diameter bars in the compression zone.

Table (1) Tested Beam Details.

Group No.	Beam label	V_f %	l_f / ϕ_f	Main reinforcement	μ/μ_{max} reinforcement ratio
A	B1	0	0	3 ϕ 16	0.30
	B2	0.10	68	3 ϕ 16	0.30
B	B3	0.10	68	4 ϕ 16	0.45
	B4	0.10	68	5 ϕ 16	0.60
C	B5	0.05	68	3 ϕ 16	0.30
	B6	0.2	68	3 ϕ 16	0.30
D	B7	0.10	42	3 ϕ 16	0.30
	B8	0.10	26	3 ϕ 16	0.30

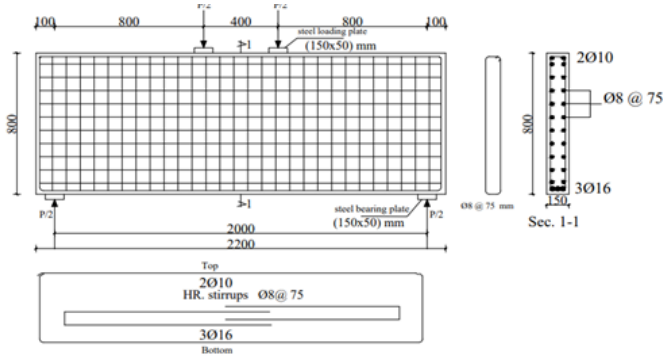

(a) Beams B1, B2, B5, B6, B7 and B8

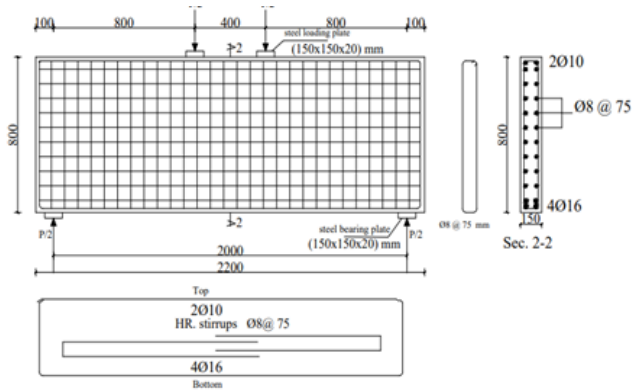

(b) Beam B3.

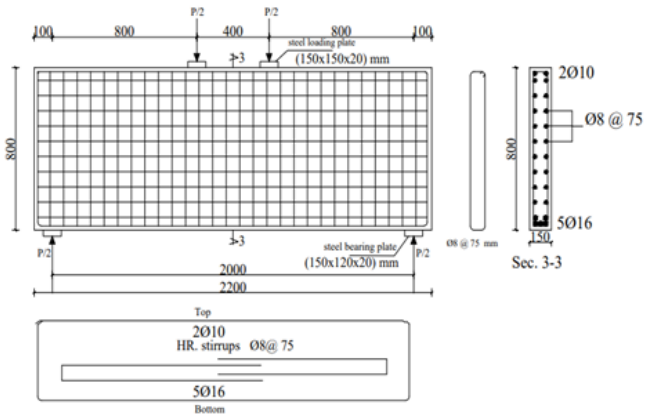

(c) Beam B4

Fig. 1 Details of Tested Beams with Dimensions (150x800x2200) mm.

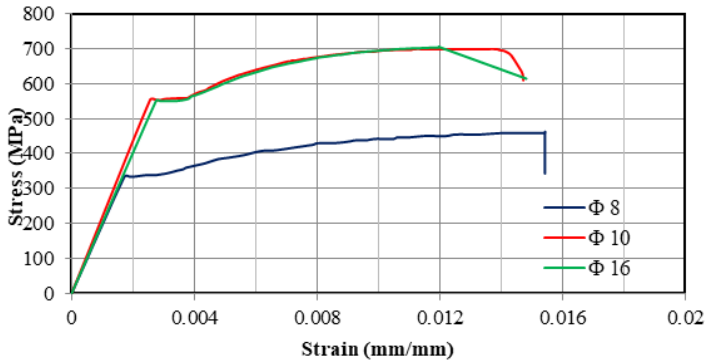

Fig. 2 Steel reinforcement typical stress-strain curves.

Table (2) Concrete Mechanical Properties

Beam	Cubic Compressive Strength, f_{cu} (MPa)	Cylindrical Compressive Strength, f_c` (MPa)	Tensile Splitting Strength, f_t (MPa)	Strain at Maximum Compressive Strength, ε_0 (-)
B1	30	24.90	2.9	0.00314
B2	33.5	27.90	3.10	0.00285
B3	33.5	27.90	3.10	0.00285
B4	33.5	27.90	3.10	0.00285
B5	31.0	25.8	3.44	0.00305
B6	37.5	30.20	3.25	0.00265
B7	33.0	27.14	3.30	0.00290
B8	32.0	26	3.12	0.00293
Average	32.9	27.2	3.15	0.00297

Table (3) Mechanical and Physical Properties of Steel Bars.

Bar Diameter (mm)	Actual Net Area (mm^2)	Yield Strength (MPa)	Strain at Yield Strength, ε_y (-)	Ultimate Strength, f_u (MPa)	Elongation % (-)	Young's Modulus, E_s (GPa)
8	48.50	332	0.00182	460	15.3	200
10	78.50	550	0.00286	690	13.7	200
16	197.98	552	0.00285	705	12.1	200

2.2 Materials properties

The mechanical properties of polypropylene fibers, reinforcing steel bars, and concrete were ascertained by experimentation, in accordance with the Egyptian Code for Design and Construction of Reinforced Concrete Structures ECP203-2017 [1]. The coarse aggregate in the experimental program was well-graded dolomite. The dolomite that is used has a specific gravity of 2.65 kg/m3 and a size range of 10 to 20 mm as shown in fig. 3. The fine aggregate had a specific gravity of 2.63 kg/m3 and was nearly pure sand. The foam employed in this study has a specific gravity of 0.07 kg/liter and a diameter of 1-3 mm. Because it prevents concrete gases from leaking, the use of foam processors in mixed designs is one of the most crucial elements in maintaining resistance and compressive strength over an extended length of time. Fig. 4 shows the foam configuration shape. The silica fume percentage in this experimental program was 9% of the cement's weight. It is not possible for the silica fume effect to increase compressive strength by more than 15%. Sika Air satisfies the ASTM C-260 specifications for air-entraining admixtures. The lubricating effect of the tiny bubbles in concrete increases workability and playability. The Sika air content in the mix design is displayed in Table (4). After 28 days, lightweight concrete was designed with nominal cubic (f_{cu}) and cylindrical (f_c) strengths of 36 and 30 MPa, respectively. Table 4 lists the ingredient quantities required for one cubic meter of concrete mix.

Table (4) Concrete Mix Design: Proportions per Cubic Meter

Cement (kg)	Sand (kg)	Aggregate (kg)	Sika Air (kg)	Silica Fum (kg)	Foam (kg)	Super-Plasticizer (kg)	Water (kg)
455	404	526	0.75	53	21.2	5.1	190

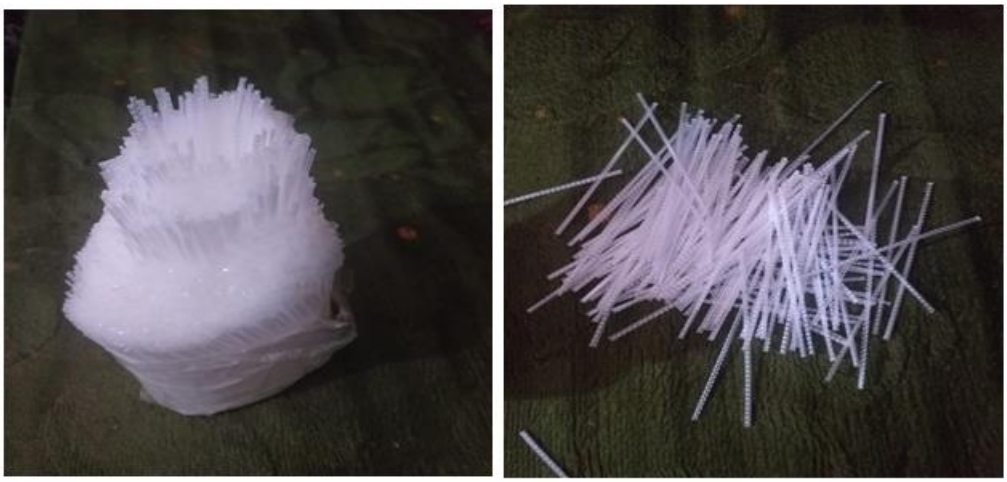

Fig. (3) Polypropylene Fiber

Figure (4) shows foam configuration shape

2.3 Instrumentation and test procedure

The experimental setup involved testing all specimens under two-point loading conditions, with a 2000 mm clear span and 800 mm shear span. A hydraulic jack, as shown in Fig. 5, applied the load at two points with a 400 mm spacing. A load cell, secured to the testing frame using plates and high-strength steel bolts, recorded the applied force. The specimens were supported by steel bearing plates placed on a steel I-section. During the test, cracks were marked at each load increment. To monitor deflections, three Linear Variable Differential Transducers (LVDTs) were positioned at the third points of the span, as depicted in Fig. 5. The specimens had external measuring devices attached to them in order to measure the crack propagation, applied vertical stresses, and overall deformations. LVDTs attached to the beam recorded the deflected shape of the beam during the test phases. To record every result throughout the test phases, the load cell and LVDTs were connected to the data logger system.

Fig. 5 Test set-up and instrumentation.

3. Experimental Results

3.1 Visual Cracking Pattern Analysis

Fig. 6 illustrates the crack patterns observed in all tested beams. For the deep beam B1, where B1 is the control specimen without Polypropylene fibers. The first flexural crack was observed at mid-span at a load level of 23.5 t. The first diagonal shear crack was observed at a load level of 25 t, as shown in Table 5. The corresponding deflection at the first flexural crack was 1.12 mm. Shear-compression failure occurred when the inclined crack further propagates upwards, and then the concrete above the crack fails by crushing, accompanied by a loud noise. The first shear cracks, observed as either diagonal or inclined, formed in the shear span close to the support. As the applied load increased to a range of 29% and 39% of the ultimate load, bending moments induced these cracks. However, importantly, crack propagation was limited, and they did not extend into the compression zone.

Between 39% and 49% of the ultimate load, the cracks transitioned, inclining towards the central zone to establish the primary diagonal crack, which functioned as the main diagonal concrete strut. Upon reaching approximately 75% of the ultimate load, the progression of cracking changed; instead of new cracks, the existing diagonal cracks widened substantially, growing from 0.50 mm to 2 mm, and this led to the crushing of the diagonal strut.

The analysis indicates that increasing the polypropylene fiber (PF) content in the concrete specimens enhances compressive strength, as demonstrated by the comparison between specimens B2 and B6, which contain 0.1% and 0.2% PF by volume, respectively, as shown in Table 1. A higher PF volume fraction also leads to an increase in the first cracking load, although it is accompanied by a reduction in the ultimate load. Notably, specimen B6 exhibited a 28.67% increase in ultimate load and a 23.07% increase in the first flexural cracking load compared to specimen B2. Furthermore, as the PF content increases, the secant stiffness decreases, while ductility improves, consistent with findings reported in [24].

3.2 Failure modes

Figure 6 illustrates the crack patterns for all tested beams. Beam B1 exhibited a brittle shear failure. Beams B2-B6 failed in shear with warning signs, including concrete splitting between the load pad and support. Beams B7 and B8 showed splitting as the main crack propagated, dividing the beam from the loading plate to the supports.

3.3 Load deflection curves and ultimate loads

As illustrated in Figure 7, the load-deflection curves for all tested beams exhibit a near-linear relationship during the uncracked phase, transitioning to nonlinear behavior following the initiation of the first crack. As (V_f%) increased from 0.0% to 0.2%, the final deflection increased by 44 % at the ultimate load. Increasing fiber volumetric percent (V_f%) improves the beam stiffness at different levels of loads. Increasing the main steel reinforcement ratio significantly enhanced beam stiffness across various loading stages. For beam B3, the peak load and maximum deflection increased by 30.61% and 32.32%, respectively, while beam B4 showed corresponding increases of 39.42% and 35.02% compared to the control specimen B1. Additionally, increasing the fiber volumetric content (V_f) had a notable impact on the ultimate load-carrying capacity ($Pu_{(EXP)}$). In specimen B5, an increase in V_f from 0.0% to 0.05% resulted in a 9% rise in $Pu_{(EXP)}$. When V_f was further increased to 0.2% in specimen B6, $Pu_{(EXP)}$increased by 33%. The maximum deflections (Δ_{max}) observed were 3.34 mm for B5 and 4.72 mm for B6. Specimen B7 achieved a peak load of 69.5 t, reflecting an 11.38% increase over the control. Meanwhile, specimen B8 recorded the highest maximum deflection at peak load, measuring 5.45 mm, representing an 83.5% increase relative to specimen B1.

Table (5) Experimental Results.

Group	Beam label	P_{crfm} (ton)	P_{crs} (ton)	$P_{u\ exp.}$ (ton)	$\Delta_{u\ exp.}$ (mm)
A	B1	23.5	25	62.400	2.97
	B2	26	32	71.500	3.64
B	B3	28	33.5	81.500	3.93
	B4	29.5	37.5	87	4.01
C	B5	23	27.5	68.500	3.34
	B6	32	36	92	4.72
D	B7	25.0	28	69.500	4.68
	B8	24.4	29	67.300	5.45

Where:

$P_{crfm:}$: Load at first flexural crack;

P_{crs}: Load at first diagonal shear crack;
$P_{u\ exp.}$: Measured ultimate load; and
$\Delta_{u\ exp.}$: Measured ultimate deflection.

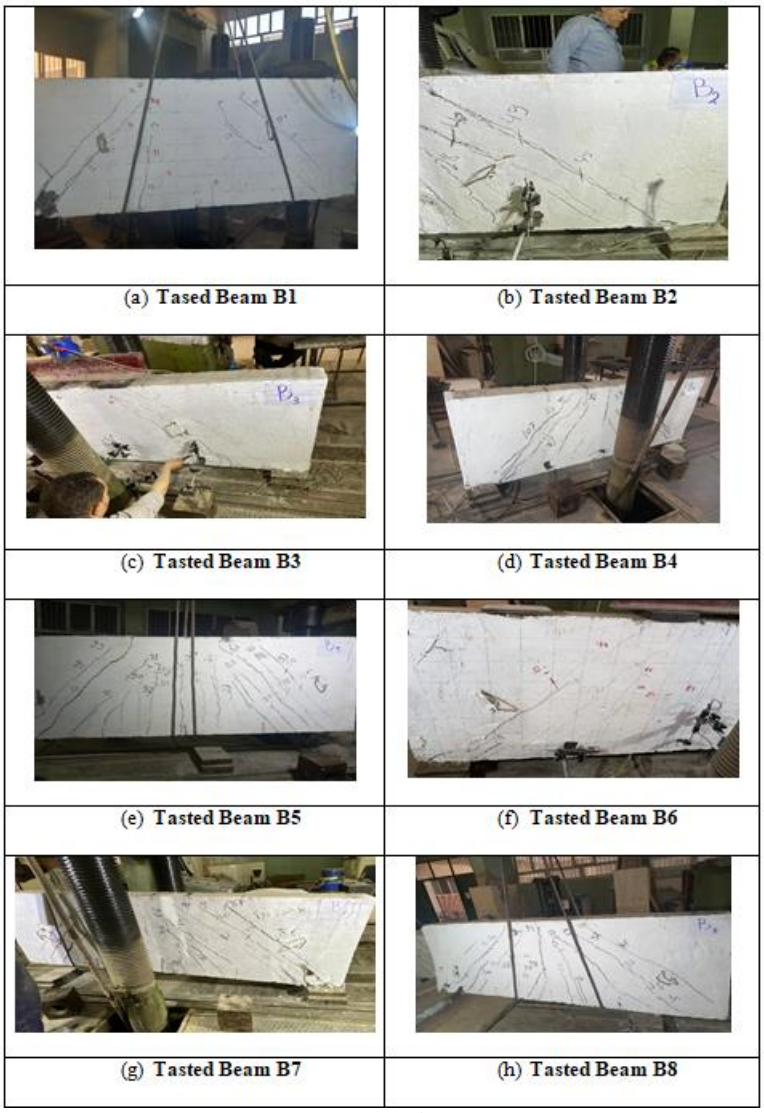

Fig. 6 Cracking patterns for tested beams.

4. Numerical Analysis

To predict numerically the behavior of lightweight reinforced concrete (LWRC) deep beams with Polypropylene fibers, ANSYS V15 [25] computer nonlinear finite element program was employed. Table 6 presents the element properties used in the simulation model. The numerical predictions were then compared with experimental results, as documented in Table 7. One of the main advantages of using a software program is to eliminate the need for the cost of making many specimens in an experimental program, and saving time. It can also be used to predict the behavior of steel reinforcement before and after yielding and concrete behavior pre- and post-cracking.

LINK 180 is a three-dimensional element with two nodes that are used for modeling the steel reinforcement and stirrups [25]. As shown in Figure 7a, each node possesses three degrees of freedom: translation in the x, y, and z directions. SOLID65 is a three-dimensional element with 8 nodes that is used for modeling reinforced concrete. As illustrated in Figure 7.b, this element has three degrees of freedom per node: translation in the X, Y, and Z directions. SOLID 185 is a three-dimensional element with eight nodes, which are used for modeling top and bottom steel plates (loading and bearing plates). The three degrees of freedom per node, involving translation in the x, y, and z directions, are specified in Table 6. Lightweight concrete is modeled using the SOLID65 element. Its behavior includes both linear and nonlinear characteristics. Nonlinear constitutive material relations are used for lightweight concrete modeling in compression and tension, more details can be found in [26]. In the linear range, concrete is considered as isotropic material up to the point of cracking. Beyond this, in the nonlinear stage, concrete exhibits plasticity. In tension, cracking can occur at each integration point in three orthogonal directions. The material properties for the elements SOLID65, LINK180, and SOLID185 are provided in Table 6.

Figure 8 illustrates the comparison between experimental results and nonlinear finite element (FE) analysis,

demonstrating a strong correlation. The mean agreement for cracking load, ultimate load, and displacement at ultimate load was 99.62%, 102.48%, and 102.6%, respectively, with a standard deviation of less than 2.2%, as summarized in Table 7. Similarly, Figure 9 presents the deformed shapes and stress contours of all tested beams. The comparison of experimental data with nonlinear FE analysis performed using ANSYS Version 15 further confirms this consistency, with mean agreement values of 95.98% for cracking load, 100.72% for ultimate load, and 102.15% for displacement at ultimate load, and a standard deviation below 9.1%.

An increase in the main steel reinforcement ratio was found to enhance crack control and increase the ultimate load capacity. Both the reinforcement ratio and the polypropylene fiber (PF) volumetric content significantly influenced the cracking load, ultimate load, and displacement ductility of lightweight reinforced concrete deep beams. Specifically, increasing the main reinforcement ratio by 50% and 100% led to improvements in cracking load by 3.83% and 8.43%, and in ultimate load by 14.24% and 19.82%, respectively.

The incorporation of polypropylene fibers also demonstrated marked improvements in structural behavior. For beam B2 with 0.1% PF content, the first crack load increased by 6.53%, the ultimate load capacity by 7.8%, and displacement at ultimate load by 8.9%, compared to a beam without fiber. When the PF content was increased to 0.2% (beam B6), the first crack load increased by 32.65%, the ultimate load capacity by 48.97%, and the displacement at ultimate load by 61.64%. Moreover, the experimental and numerical values for deflection at ultimate load (Δu) were nearly identical, with a Δu(EXP) / Δu(FE) ratio of 102.15%, indicating excellent agreement between test results and simulation.

Table (6) ANSYS Model Element Properties.

Element Classification	Application (Type)	Real Constant	Steel Section Area	Material
Solid 65	Concrete Elements	-----	-------	1
Link 180	Steel Bars	Set 1	A_{S1}	2
		Set 2	A_{S2}	3
	Stirrups	Set 4	A_{S3}	4
Solid 185	Plates	-------	-------	5

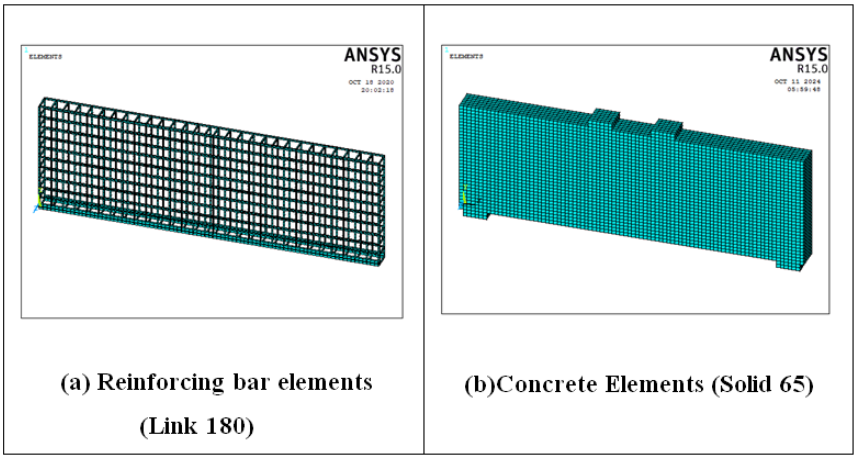

Fig. 7 ANSYS Modeling of Deep Beams

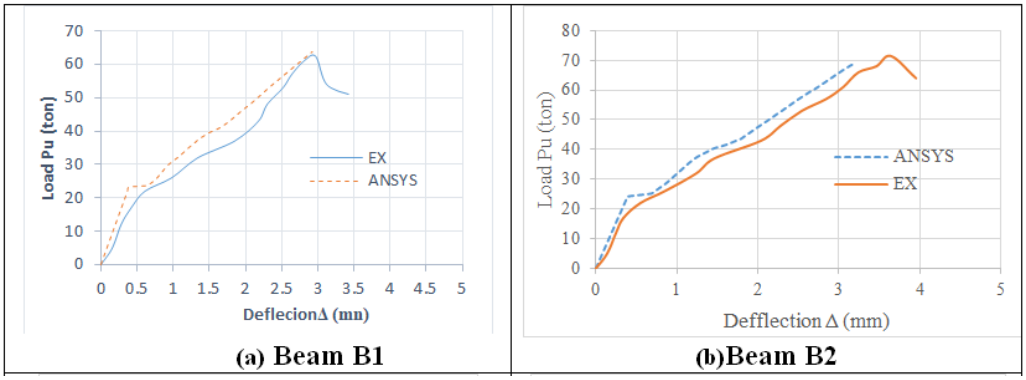

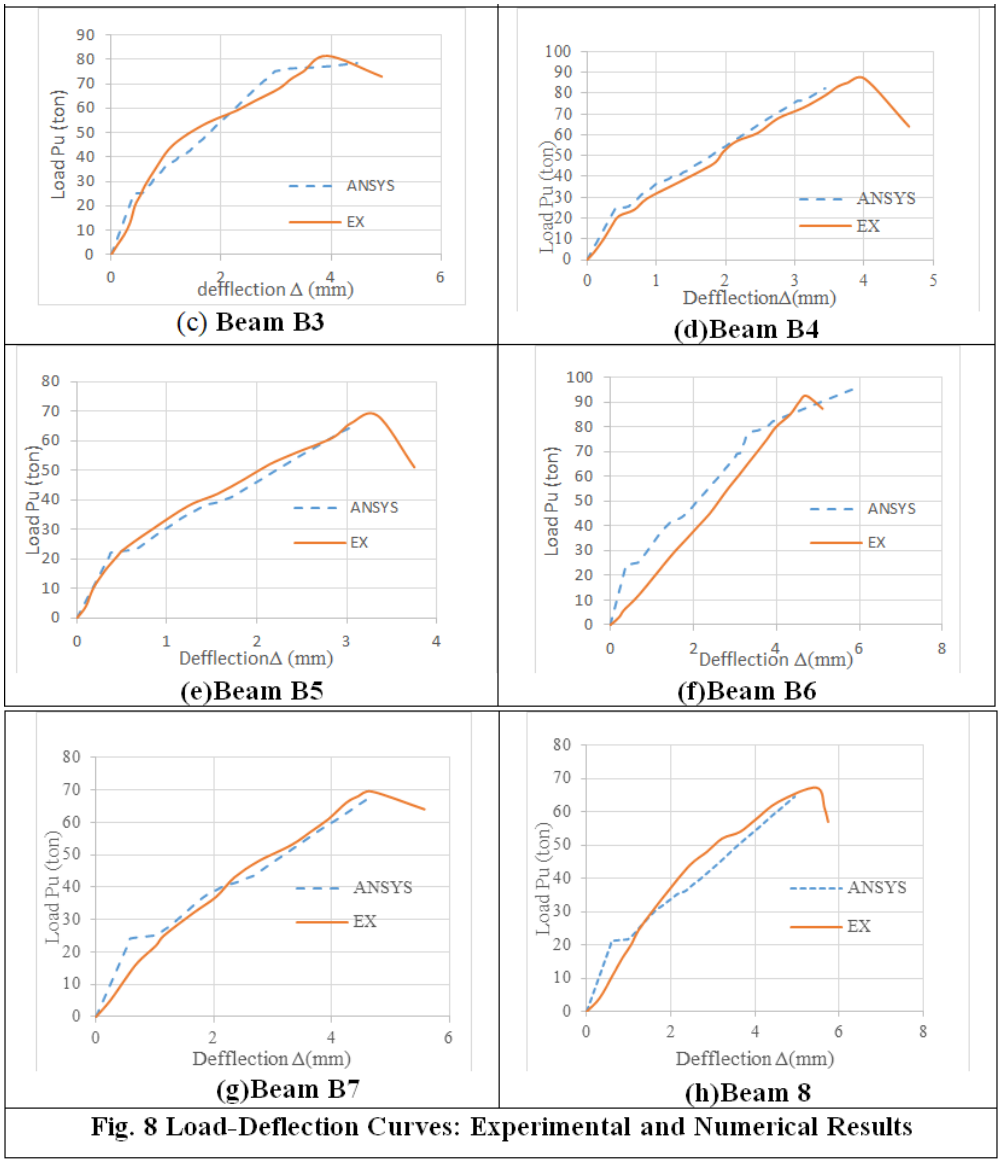

Fig. 8 Load-Deflection Curves: Experimental and Numerical Results

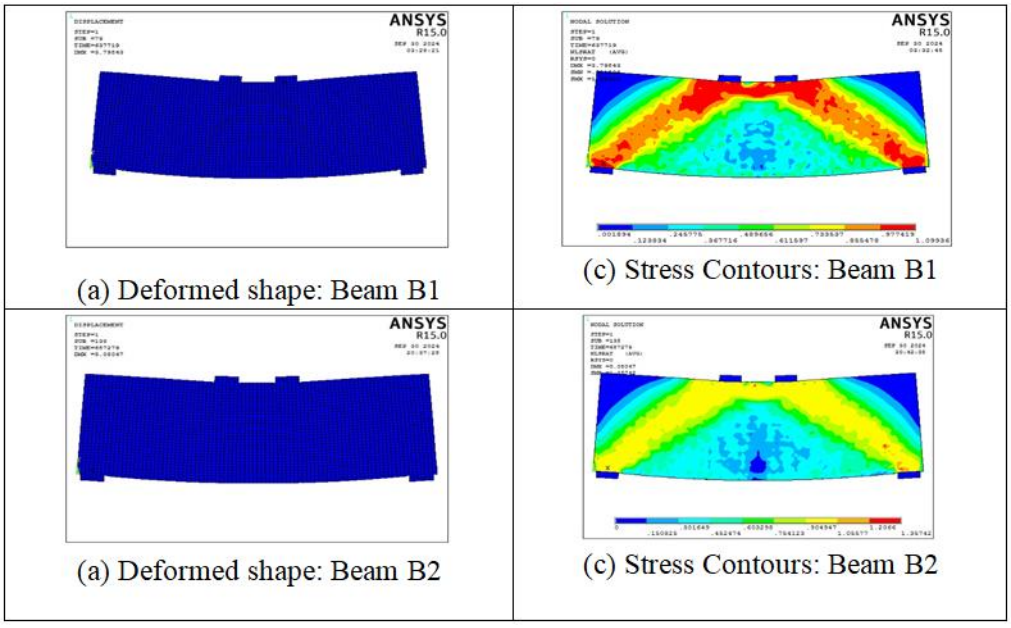

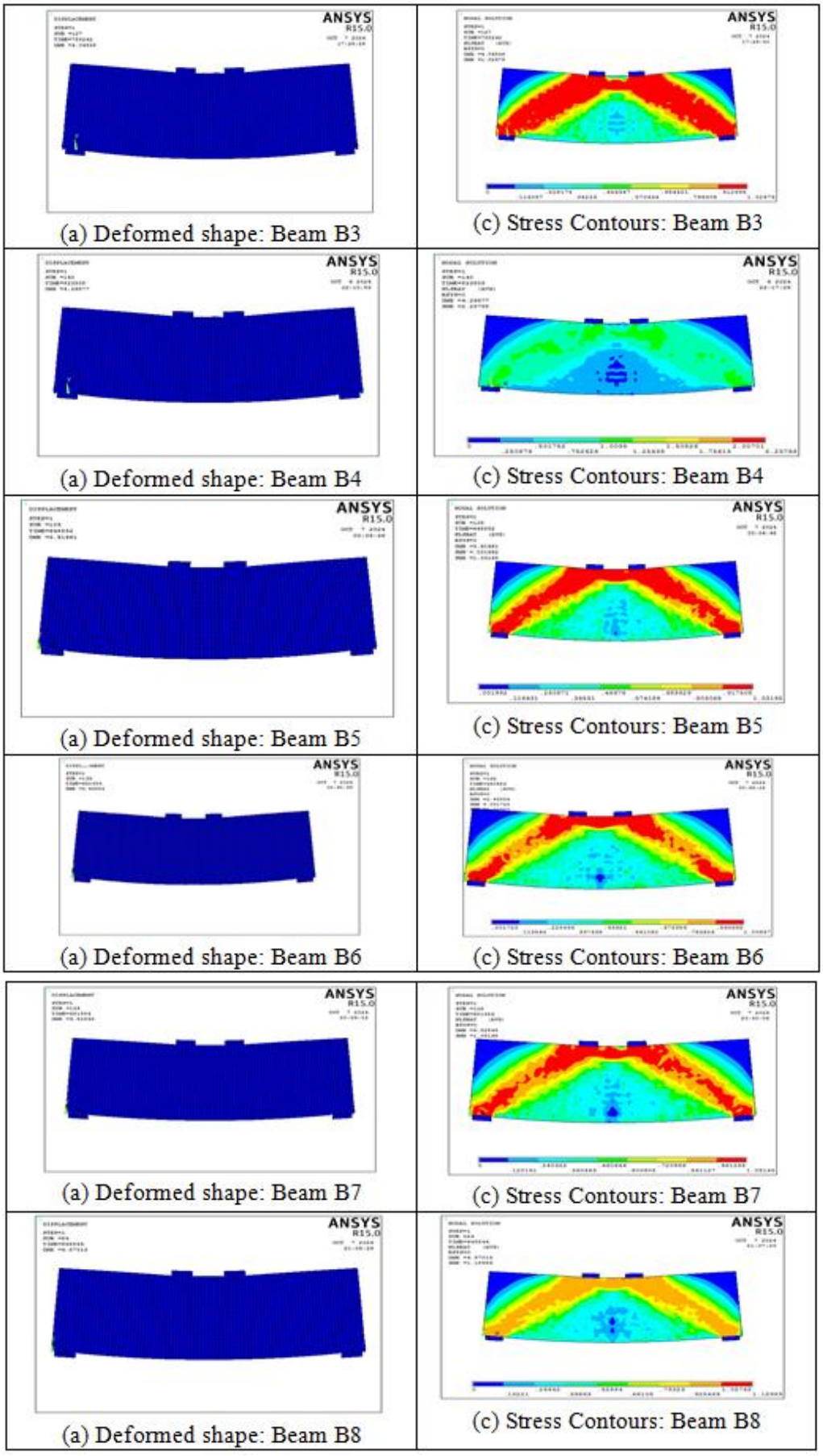

Fig.9 Deformation and Stress Contours in Tested Beams

Table (7.) Finite Element Analysis Results (FE).

Group No.	Beam No.	$P_{crf\,FE}$ (ton)	$P_{crs\,FE}$ (ton)	$P_{u\,FE}$ (ton)	$\Delta_{u\,FE}$ (mm)	$\frac{P_{crf\,FE}}{P_{crf\,exp.}}$ % (-)	$\frac{P_{crs\,FE}}{P_{crs\,exp.}}$ % (-)	$\frac{P_{u\,FE}}{P_{u\,exp.}}$ % (-)	$\frac{\Delta_{u\,FE}}{\Delta_{u\,exp.}}$ % (-)
A	B1	24.5	28.5	63.77	2.92	104.25	114	102.19	98.31
	B2	26.1	30.2	68.73	3.18	100.38	94.37	96.12	87.36
B	B3	27.1	32.1	78.52	4.47	96.78	95.82	96.34	113.74
	B4	28.3	35.4	82.35	3.44	95.93	94.40	94.65	85.78
C	B5	23.9	29.3	64.88	3.06	103.91	106.54	94.71	91.61
	B6	32.5	36.7	95	4.72	101.56	101.94	103.26	100
D	B7	25.1	28.5	6815	4.70	100.4	101.78	98.05	100.42
	B8	24.1	28.1	64.58	4.94	98.77	96.89	95.95	90.64
Mean						95.98	97.66	100.72	102.15
S.D %						9.10	3.30	6.80	6.40

5. Conclusions

1- Compared to a control beam (B1) without fibers, incorporating 0.2% Master Fiber 154SPA (Polypropylene fiber) in reinforced concrete lightweight deep beams (Beam B6) resulted in significant improvements: a 36% increase in first crack load, a 32.17% increase in ultimate load capacity, a 30.55% increase in first diagonal shear crack load, and an 11.2% increase in displacement ductility.

2- By increasing the main steel reinforcement ratio, crack width control was enhanced in beams B3 and B4, leading to ultimate load increases of 12.3% and 17.8% compared to control specimen B2.

3- Increasing the main reinforcement ratio by 33% and 66% resulted in a 7.14% and 11.86% increase in cracking load, a 12.3% and 17.8% increase in ultimate load, and an 8.7% and 12.26% increase in displacement ductility, respectively.

4- Increasing the Polypropylene fiber volumetric percentage (Vf %) by 100% resulted in a 36% increase in first crack load, a 32.17% increase in ultimate load, and an 11.2% increase in displacement ductility. Conversely, a 50% decrease in Vf % resulted in an 11.53% decrease in first crack load, a 4.2% decrease in ultimate load, and a 5.88% decrease in displacement ductility.

5- Comparison between experimental and nonlinear finite element results (ANSYS V15) demonstrates good agreement. The mean values for cracking load, ultimate load, and displacement at ultimate load were 99.62%, 102.48%, and 102.6%, respectively, with a standard deviation of less than 2.2%, as shown in Table 7.

6- During failure testing, all mixes incorporating Polypropylene fiber demonstrated enhanced performance relative to the fiberless control beam. Fibrous beams displayed shear failure with precursory warnings and noticeable flexural cracking, while the non-fibrous beam failed abruptly in brittle shear.

REFERENCES

[1] Egyptian Code of Practice for Design and Construction of Reinforced Concrete Structures ECP-203, Housing and Building Research Center, Ministry of Building and Construction, Giza, Egypt, 2017, Chapter 6, pp. 113-122.

[2] ACI Committee 318-19, Building Code Required for Reinforced Concrete, (ACI 318-19) and Commentary (ACI 318R-19), American Concrete Institute, Farmington Hills, Mich,2018.

[3] Khalesi, M., Mirdar, S., & Samadi, A. Reduction of Tumor Necrosis Factor Alpha and Nuclear Factor-Kappa B Gene Expression in Lung Tissue of Rats After a Period of Swimming Training. Sport Physiology, 10(37), 153-166. (2018)

[4] Aziz, M. A., Paramasivam, P., & Lee, S. L. Prospects for natural fibre reinforced concretes in construction. International Journal of Cement Composites and Lightweight Concrete, 3(2), 123-132. (1981).

[5] Madhavi, T. C., Raju, L. S., & Mathur, D. Polypropylene fiber reinforced concrete-a review. International journal of emerging technology and advanced engineering, 4(4), 114-118. (2014)

[6] Bagherzadeh, R., Pakravan, H. R., Sadeghi, A. H., Latifi, M., & Merati, A. A. An investigation on adding polypropylene fibers to reinforce lightweight cement composites (LWC). Journal of Engineered Fibers and Fabrics, 7(4), 155892501200700410. (2012).

[7] Patel, M. J., & Kulkarni, S. M. Effect of polypropylene fiber on the high strength concrete. Journal of information, knowledge and research in civil engineering, 2(2), 127. (2012).

[8] Ramadevi, K., & Venkatesh Babu, D. L. Flexural behavior of hybrid (steel-polypropylene) fibre reinforced concrete beams. European Journal of Scientific Research, 70(1), 81-87.2012)).

[9] Thirumurugan, P., Ramkumar, D., Batri, K., & Siva Sundhara Raja, D. Automated detection of glioblastoma tumor in brain

magnetic imaging using ANFIS classifier. International Journal of Imaging Systems and Technology, 26(2), 151-156. (2016).

[10] Chen, B. L., Peng, J., Li, Q. F., Yang, M., Wang, Y., & Chen, W. Exogenous bone morphogenetic protein-7 reduces hepatic fibrosis in Schistosoma japonicum-infected mice via transforming growth factor-β/Smad signaling. World Journal of Gastroenterology: WJG, 19(9), 1405.2013)).

[11] Hassoun, M. N., and Al-Manaseer, A., "Shear and Diagonal Tension in Reinforced Concrete - Mechanism and Design - 5th Edition", John Wiley & Sons, Inc., New Jersey, USA, May 2012, pp.251-299.

[12] Kong, F. K., "Reinforced Concrete Deep Beams", Taylor & Francis Books, Inc., Bishopbriggs, Glasgow, U.K, Apr. 2002, pp.5-22.

[13] Mihaylov, B. I., Hunt, B., Bentz, E. C., and Collins, M. P., "Three-Parameters Kinematic Theory for Shear Behavior of Continuous Deep Beams ", ACI Structural Journal, V. 112, No. 1, Jan. 2015, pp. 47-58.

[14] Tang, C. T., and Tan, K. H., "Interactive Mechanical Model for Shear Strength of Deep Beams", Journal of Structural Engineering, ASCE, V. 130, No.10, Oct. 2004, pp.1534-1544.

[15] Fanella, D. A., & Naaman, A. E. Stress-strain properties of fiber reinforced mortar in compression. In Journal Proceedings (Vol. 82, No. 4, pp. 475-483). (1985, July).

[16] Minnaugh, P. L., "The Experimental Behavior of Steel Fibers Reinforced polymers Retrofit Measures", M.Sc. Thesis, University of Pittsburgh, School of Engineering, Pennsylvania, U.S.A. 2006.

[17] Pendyala, R., Mendis, P., and Patnaikuni, I., "Full Range Behavior Flexural Members: Comparison of Ductility Parameters of High and Normal- Strength Concrete Members", ACI Structural Journal, V.93, No.1, Jan. 1996, pp.30-35.

[18] Abd, E. A. A. E. A. PERFORMANCE OF STEEL FIBERS REINFORCED CONCRETE DEEP BEAMS (Doctoral dissertation, Benha University).2015)).

[19] Campione, G., La Mendola, L. and Zingone, G., "Strength and Ductility of High Strength Fiber Reinforced Concrete Circular Columns Subjected to Eccentric Loads", First European Conference Earthquake Engineering, Parigi, 1998.

[20] Campione, G., Miraglia, N. and Papia, M., "Mechanical Properties of Steel Fiber Reinforced Lightweight Concrete with Pumice Stone or Expanded Clay", Materials and Structures, 34(238), 2001, 34.4: 201-210.

[21] S Manharawy, M., A Mahmoud, A., H El-Diasity, M., & O El-Mahdy, O. (2021). Shear Performance of Steel Fibers Lightweight RC Deep Beams: Numerical and Analytical Study. Engineering Research Journal (Shoubra), 50(1), 93-105.

[22] Manharawy, M. S., Mahmoud, A. A., El-Mahdy, O. O., & El-Diasity, M. H. (2022). Experimental and numerical investigation of lightweight foamed reinforced concrete deep beams with steel fibers. Engineering Structures, 260, 114202.

[23] Lim, S.K., Tan, C.S., Li, B., Ling, T., Hossain, M.U. and Poon, C.S., "Utilizing high volumes of quarry wastes in the production of lightweight foamed concrete", ", Journal of Construction Building Materials, 2017, 151, 441–448.

[24] Alshannag, M., Alshmalani, M., Alsaif, A., & Higazey, M. (2023). Flexural performance of high-strength lightweight concrete beams made with hybrid fibers. Case Studies in Construction Materials, 18, e01861.

[25] ANSYS 15 Manual Set, ANSYS Inc. South pointe technology drive, Manager, PA, USA. 2015 https://forum.ansys.com/uploads/846/SCJEU0NN8IHX.pdf.

[26] Abd ELRAHEM, A. M. "Behaviour of Light Weight Reinforced Concrete Deep Beams", M.Sc. Thesis to be submitted, Faculty of Engineering at Shoubra, Benha University, 2025.